SEMARAK ILMU PUBLISHING

CFD Letters

Journal homepage:
https://semarakilmu.com.my/journals/index.php/CFD_Letters/index
ISSN: 2180-1363


# Performance Evaluation of Square Cyclone Separator with Cone Geometry Variations

Fredy Surahmanto[1,*], Aji Pamungkas[1], Dhimas Agung Mutoha[1], Arianto Leman Soemowidagdo[1], Beni Tri Sasongko[1], Sukardi Sukardi[1], Raihan Lutfianto[2], Muhammad Rizky Pratama Hakim[2]

[1] Department of Mechanical Engineering Education, State University of Yogyakarta, Indonesia
[2] CADFEM SEA Pte. Ltd., Singapore

**ARTICLE INFO**

***Article history:***
Received 12 September 2023
Received in revised form 15 October 2023
Accepted 11 November 2023
Available online 29 February 2024

***Keywords:***
Computational Fluid Dynamics; Dual Inverse Cone; Single Cone; Square Cyclone Separator

**ABSTRACT**

Rapid industrial development with intensive operations increases exhaust emissions that are polluting the environment and human health. Efforts to overcome the problem are urgent to be realized, one of which is by using a particle separator such as a cyclone separator. Along with that, the design of a cyclone separator with the best performance is very important. Therefore, it is necessary to innovate and analyze the design of the cyclone separator by varying the cone geometry of the cyclone. This study aimed to determine the best square cyclone separator among square cyclone separators with various cone geometries, including single cone, dual inverse cone 1, and dual inverse cone 2. It was conducted by Computational Fluid Dynamics (CFD) simulation and experiments and then continued by comparing pre-determined aspects comprising pressure drop, collection efficiency, static pressure contours, tangential velocity contours in the cyclone body, tangential velocity vectors in the cone geometry, and tangential velocity vectors at the cyclone inlet. The single cone is the best among all cone variations since it fulfils more aspects better than the dual inverse cones, namely: dominantly lowest pressure drop of 188.5 Pa, static pressure contour of 10.42 Pa, tangential velocity contour of 3.06 m/s, flow direction of the tangential velocity vector in the cyclone geometry was at the centre of the bin, and flow direction of the tangential velocity vector at the cyclone inlet was parallel.

## 1. Introduction

The rapid development of the industry with very intensive operations, in addition to bringing positive impacts, also harms environmental and human health in the form of increased exhaust emissions containing polluting substances. For example, the use of boilers in the industry to produce hot steam through the combustion process will produce flue gas emissions containing pollutants in the form of solid particulates and residual gases such as $NO_2$ and $SO_2$. The percentage of solid particulates remaining from this combustion is very high, which is about 5% of the total weight of the fuel used [1, 2].

* *Corresponding author.*
*E-mail address: fredy_surahmanto@uny.ac.id (Fredy Surahmanto)*

https://doi.org/10.37934/cfdl.16.7.136149

Flue gas emissions from combustion residues, especially solids in the form of bottom ash and fly ash, must be handled seriously so that they do not become a problem for workers and the community because they are very small and vary in size up to ± 10 µm [3, 4]. It is found that tiny particles if inhaled by humans, will cause irritation and pneumoconiosis [5]. Therefore, the handling of flue gas emissions needs to be focused on considering its dangerous impact on health. Meanwhile, the use of chimneys to emit flue gas from boilers is not optimal, because previous research shows that the higher the chimney, the more gas emissions will spread [6]. Equipment that can help minimize the increase in solid particles in exhaust emissions is a cyclone separator.

A Cyclone separator is a device used to separate solid particulates before being released freely into the air by utilizing centrifugal force [7]. Compared to other types, cyclone separators are used in many industrial processes because of the many advantages obtained such as ease of manufacture, simplicity, low production costs, high-efficiency levels, and the ability to be adapted to large processes [8].

Various shapes and sizes of cyclone separators are designed according to industry needs. However, broadly speaking, cyclone separators are categorized into square cyclone and conventional cyclone separators [9]. It is known from previous research that the square cyclone separator that has a square cross-section is easy to construct, has a fast start time and has a higher efficiency than a conventional cyclone with a round cross-section [10].

From previous studies on square cyclone separators, it is found that separators with double cones have higher efficiency than those of a single cone [9]. In this case, the CFD simulation used Reynolds Stress Model method and hexahedral mesh type. In addition, a cyclone equipped with a dustbin can produce higher efficiency [11]. However, existing research that studied square cyclone separators using a variation of cones combined with dustbins simultaneously is still limited. Therefore, this present study focuses on the square cyclone separator with a variation of cone combined with a dustbin to determine the best cone based on the analysis of collection efficiency, static pressure contours, tangential velocity contours in the cyclone body, tangential velocity vectors in cone geometry, and tangential velocity vectors at the cyclone inlet.

## 2. Methodology

### *2.1 Research Methods*

This research used an experimental method and a Computational Fluid Dynamics (CFD) simulation. The experiment was conducted on a cyclone separator with a single cone as shown in Figure 1, as a validation of its CFD simulation. The deviation of experimental results from CFD simulation was analysed and then followed by varying the cone geometry. By comparing the aspects including pressure drop, collection efficiency, static pressure, and tangential velocity, the best cone variation can be determined.

The working principle of this equipment is to flow dust particles with the help of a vibrator motor which will be sucked into the cyclone separator using a suction blower. Particles in the gas flow are pushed radially outward to the wall by centrifugal force. The gas ascends from the cyclone via a centrally positioned tube (vortex finder). The dust particles flow downward along the cylindrical and conical walls of the cyclone towards the bottom part of the cyclone, and into the dust outlet, where they are collected.

The specifications of the equipment used are a cyclone separator (according to Table 1) as the main test equipment, a vibrating motor with 15 V eccentric dynamo as a particles feeding regulator, a suction blower CKE M150R1-NO (suction capacity 1000 $m^3$/h) as a particle suction device, a digital manometer HT-1890 as a measuring device for inlet and outlet pressure differences, and dust particles (coconut charcoal powder of less than 420 microns in size) as a determinant of collection efficiency.

Experimental data collection was done twice with steps included (i) weighing the charcoal dust particles before putting them into the equipment, (ii) ensuring all components of the equipment were functional and switched on, (iii) inlet air velocity was set to 12 m/s, (iv) inserting charcoal dust particles through the vibrating motor gradually, (v) after 5 minutes, weighing the particles captured in the dustbin, (vi) recording the number of particles loaded and captured to calculate the collection efficiency.

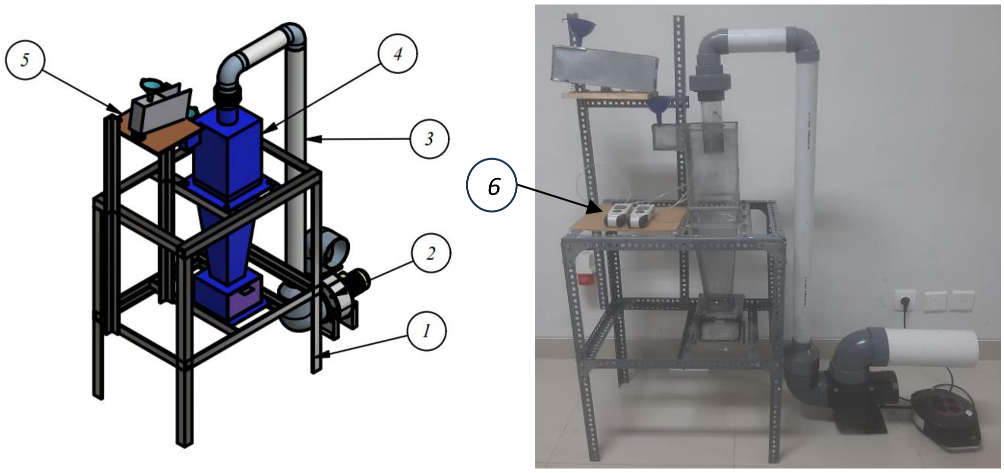


(a) (b)

**Fig. 1.** Experimental setup (a) Schematic (b) Pictorial view

Detail Equipment Setup:
1. Supporting Frame, 2. Suction Blower, 3. Pipeline, 4. Single Cone Square Cyclone Separator, 5. Vibrating Motor, 6. Manometer.

*2.2 Cyclone Geometry*

Figure 2 and Table 1 show the detailed dimensions and shapes of the cone variations:

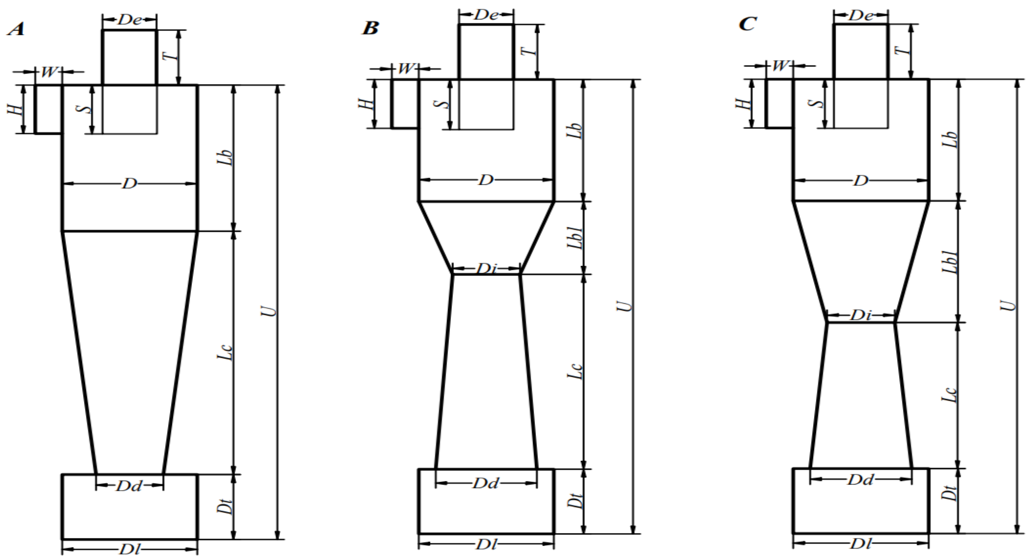


**Fig. 2.** Cone variation (a) Single cone, (b) Dual inverse cone 1, (c) Dual inverse cone 2

**Table 1**
Dimension of square cyclone separator with cone variation

| Dimension (mm) | Single cone | Dual inverse cone 1 | Dual inverse cone 2 |
|---|---|---|---|
| D | 150 | 150 | 150 |
| H | 75 | 75 | 75 |
| W | 30 | 30 | 30 |
| De | 60 | 60 | 60 |
| Di | 0 | 75 | 75 |
| S | 75 | 75 | 75 |
| Lb | 225 | 187.5 | 187.5 |
| Lb1 | 0 | 112.5 | 187.5 |
| Lc | 375 | 300 | 225 |
| U | 600 | 600 | 600 |
| B | 75 | 112.5 | 112.5 |
| T | 85 | 85 | 85 |
| Dt | 100 | 100 | 100 |
| Dl | 150 | 150 | 150 |

### *2.3 Boundary Conditions*

CFD simulation was conducted by using Fluent Mesh (with Fluent Meshing) as the input solver and varying the inlet velocity from 12 to 28 m/s and particle size from 5 to 50 µm. The numerical model used in the CFD process was the Reynold Stress Model (RSM) because it can calculate the effects of a flow line, rotation, sudden change, and vortex in a fluid [12]. The definition of boundary conditions in this present study as shown in Table 2, was based on experimental results and referred to previous research [13], while the initiation method is shown in Table 3.

**Table 2**
Boundary conditions

| Parameter | Value |
|---|---|
| Flowrate | $8.6\text{x}10^{-5}$ kg/s |
| Density | 1.225 kg/m$^3$ |
| Viscosity | $1.7894 \text{ x } 10^{-5}$ kg/m.s |
| Turbulent intensity | 5 % |
| Turbulent viscosity ratio | 10 |

**Table 3**
Initiation method

| Model condition | Model setting |
|---|---|
| Solution method | Pressure-velocity coupling: SIMPLEC |
| Spatial discretization | Pressure: PRESTO |
| | Momentum: Quick |
| | Turbulent kinetic energy: Second-order upwind |
| | Specific dissipation rate: Second-order upwind |
| | Reynolds stresses: First-order upwind |

### *2.4 Grid Independence Study*

Grid independence study was used to obtain optimum cells using poly-hexcore mesh type which was used as a reference for CFD simulation. Five grid levels were used for each cone. Figure 3 is the static pressure of a square cyclone separator with a single cone, with y = 0.14 m and an inlet velocity of 12 m/s at the radial position. Based on the grid independence study, it was known that there was no significant difference between cells 593379 and 120183. So, cells 593379 were selected as reference cells with a maximum skewness value of 0.42 (very good) and a minimum orthogonal quality of 0.21 (good). The same process was done for dual inverse cone 1 variation with reference cells 425755 and dual inverse cone 2 variation on cells 494992.

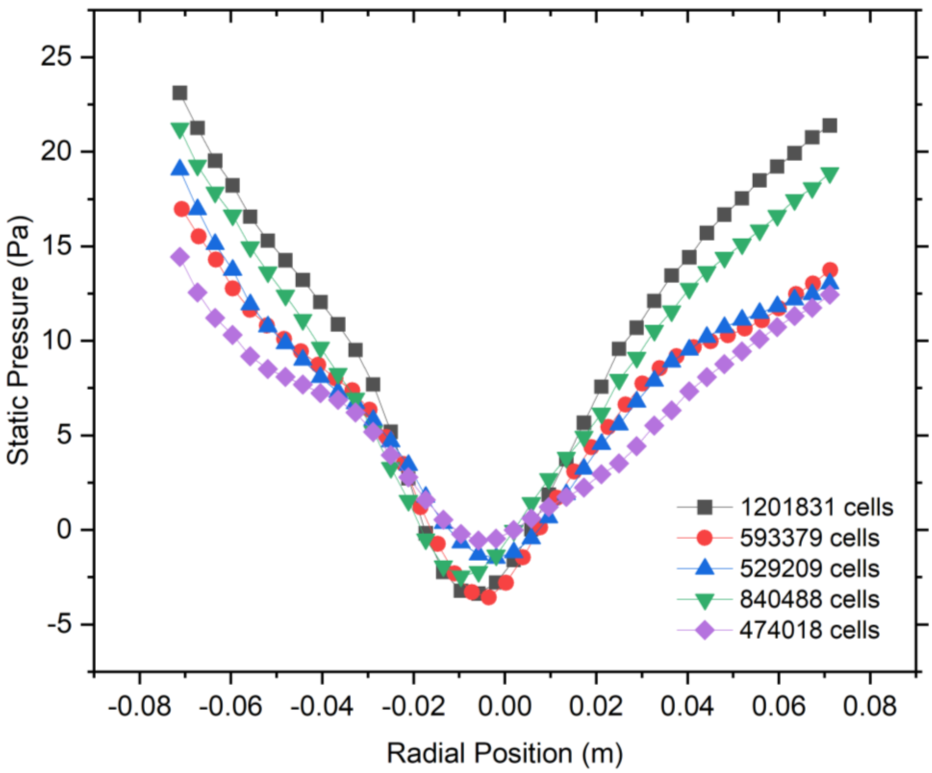


**Fig. 3.** Static pressure of a single cone at y = 0.14 m and 12 m/s inlet velocity

## 3. Results

### *3.1 Comparison of Experimental Results and CFD Simulation on Single Cone*

Experiments at a speed of 12 m/s were conducted twice with the results shown in Table 4:

**Table 4**
Experimental results at speed 12 m/s

| Run | Initial mass (g) | Captured mass (g) | Particle loss (g) | Efficiency (%) | Pressure drop (Pa) |
|---|---|---|---|---|---|
| #1 | 175.7 | 143.35 | 32.35 | 81.59 | 20.56 |
| #2 | 175.7 | 141.55 | 34.15 | 80.56 | 20.70 |

Based on both experimental data, there is a deviation between run #1 and run #2. The magnitude of the deviation of the two data is presented in Table 5:

**Table 5**
Deviation of run #1 with Run #2

| | Run #1 | Run #2 | Deviation (%) |
|---|---|---|---|
| Efficiency (%) | 81.59 | 80.56 | 1.26 |
| Pressure drop (Pa) | 20.56 | 20.70 | 0.60 |

The experiment results of the single cone show that the two runs have a deviation of 1.26 % for efficiency and 0.6 % for pressure drop. The magnitude of the deviation on the single cone is still tolerable and can be considered to be fairly precise. Deviation in efficiency is considered possible due to particles not entering the cyclone completely because some remained in the feeder after the process was finished. Deviation in pressure drop is possibly due to the inside of manometer hoses being covered with particles when taking experimental data.

Table 6 shows the deviation between the experiment and the CFD simulation. The results obtained from the comparison of efficiency and pressure drop on a single cone square cyclone separator show that there is a deviation of 2.43 % for efficiency and 4.25 % for pressure drop. The deviation is still tolerable.

**Table 6**
The deviation between the experiment and CFD simulation

| | Experiment | Simulation | Deviation (%) |
|---|---|---|---|
| Efficiency (%) | 81.08 | 83.05 | 2.43 |
| Pressure drop (Pa) | 20.63 | 21.50 | 4.20 |

### *3.2 CFD Simulation of Cone Geometry Variations*
#### *3.2.1 Pressure drop*

The pressure drop of the cyclone separator is obtained by Eq. (1), as follows:

$$\Delta P = P_i - P_o \tag{1}$$

With ΔP as the pressure drop (Pa), $P_i$ as the inlet pressure (Pa), and $P_o$ as the outlet pressure (Pa). The pressure drop is the pressure difference between two points in a device that carrying fluid. The pressure drop can happen due to the friction and the shape of the device itself. Determining the pressure drop is crucial as the higher the pressure drop, the more energy is required to maintain the desired flow. Figure 4 shows the pressure drop of the three cone geometry variations at various inlet velocities.

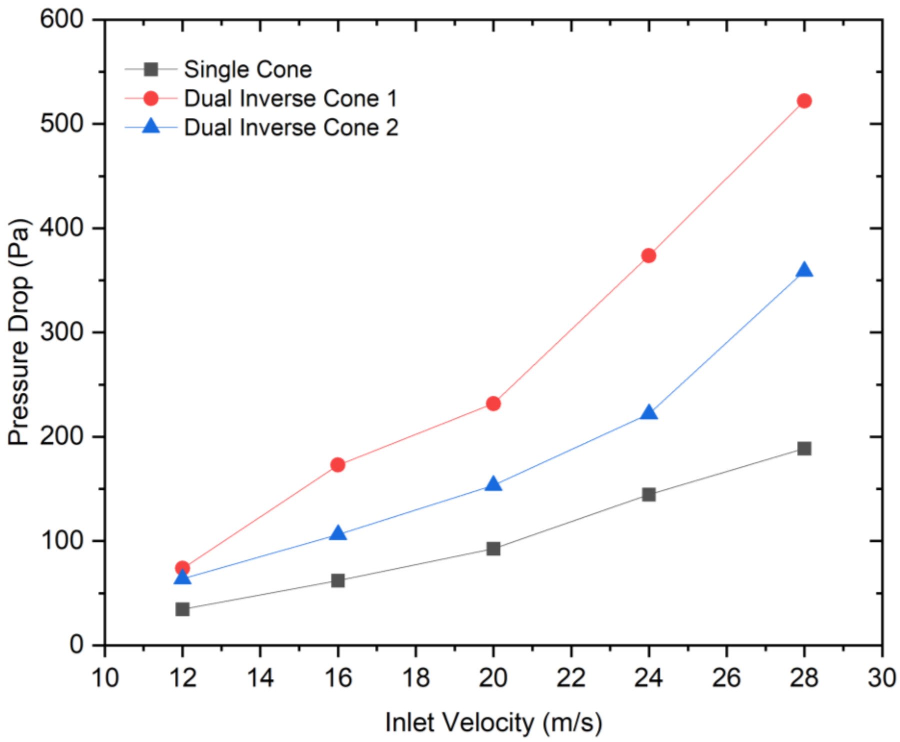


**Fig. 4.** Pressure drop with inlet velocity variation for 5 µm particle size

Based on Figure 4, it is known that from 12 m/s to 28 m/s inlet velocity, single cone, dual inverse cone 1, and dual inverse cone 2, experienced an increase in pressure drop from 34.5 Pa to 188.5 Pa, from 73.7 Pa to 522.1 Pa, and from 63.8 Pa to 359 Pa. This is in line with previous research which states that the pressure drop will increase as the inlet velocity increases [14].

### *3.2.2 Efficiency*

The efficiency of the cyclone separator can be determined by Eq. (2), as follows:

$$\eta = \frac{M_c}{M_f} \tag{2}$$

With η is the efficiency (%), $M_c$ is the captured mass (Kg), and $M_f$ is the feed mass (Kg). This efficiency represents the ability of the cyclone separator to remove dirt from the main flow.

Based on Figure 5, the collection efficiency obtained from CFD simulation on the three cones with particle size variations of 5 - 50 µm, is in the range of 85.42 % to 89.97 %. A slight difference occurs in the single cone with relatively stable efficiency. In the dual inverse cone 1, the efficiency is almost the same as the single cone but decreases more significantly at particle sizes from 5 µm to 15 µm. In the dual inverse cone 2, the efficiency is up and down significantly.

These results are quite different from a previous study where the efficiency tends to increase as particle size increases [9]. The other study shows that the efficiency increases at a size of 1.5 µm then drops to a size of 10 µm [15]. The difference between the two studies is possible because the first did not use a dustbin while the second did. So, it is found that the simulation of the present study is in line with the latter study where both used a dust bin.

Figure 6 shows the collection efficiency of the three cone geometry variations at various inlet velocities.

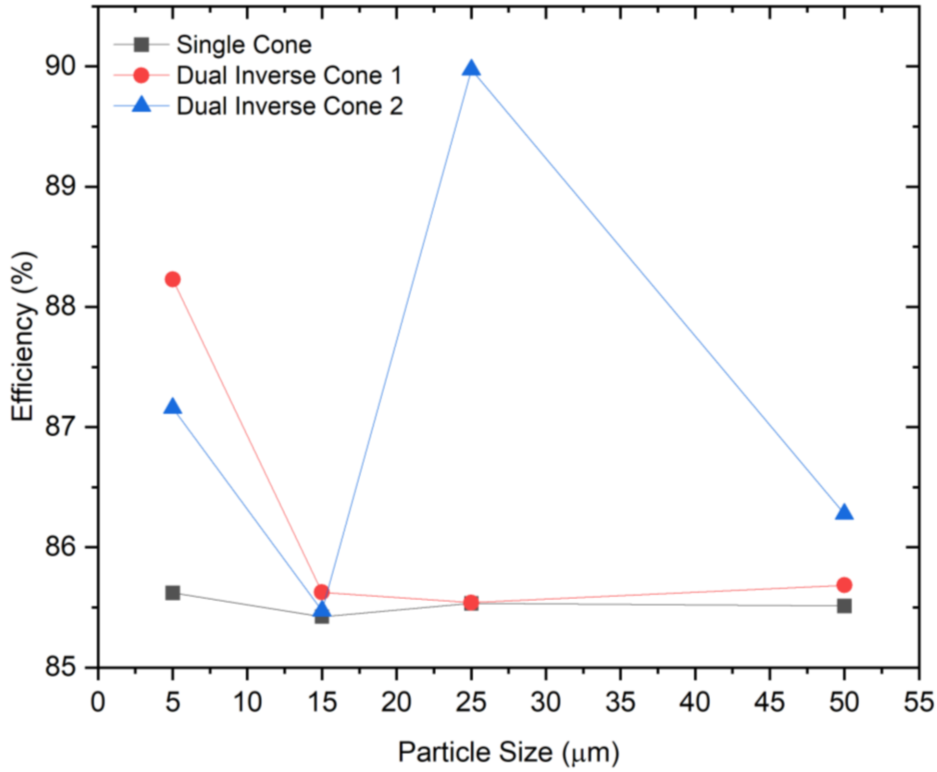


**Fig. 5.** Efficiency with particle size variation for 12 m/s inlet velocity

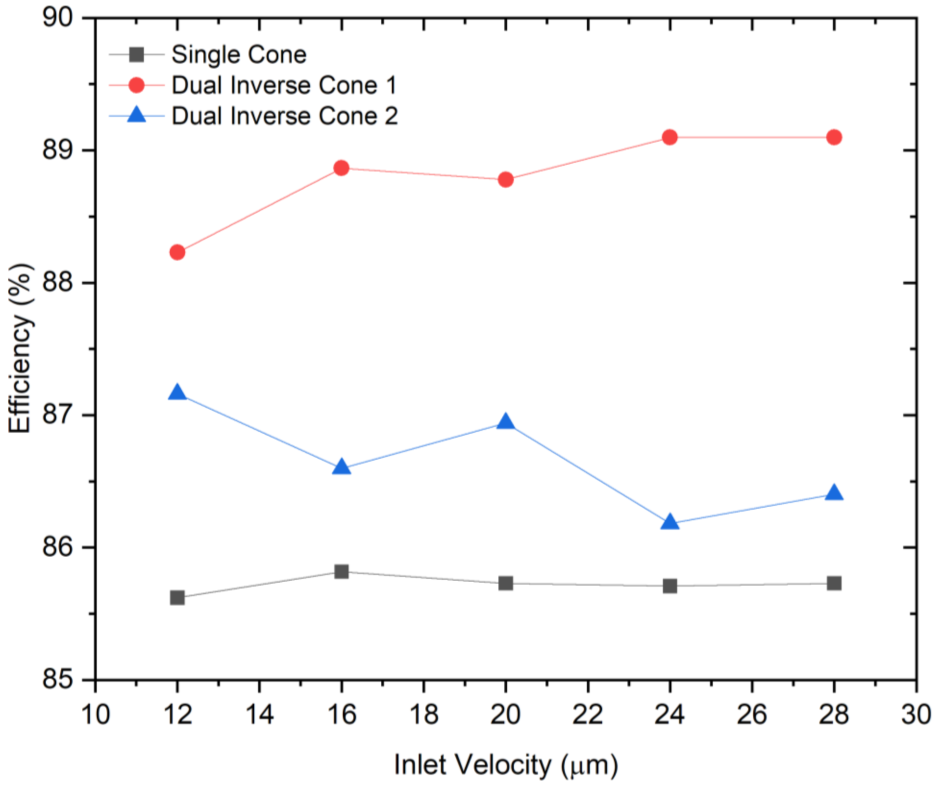


**Fig. 6.** Efficiency with inlet velocity variation for 5 μm particle size

Based on Figure 6, it is known that all geometry variations show efficiency which is in the range of 85.62% to 89.10%. However, the single cone experiences a slight increase in efficiency from an inlet velocity of 12 m/s to 16 m/s then slightly drops and tends to stabilize. This is in accordance with previous research that at increasing inlet velocity, efficiency shows an increasing trend and then slightly decreases [16].

These results are different from those obtained in dual inverse cone 1 and dual inverse cone 2 which tend to fluctuate. This is possible because the shape of the cone tip connected to the dust bin between the single cone and the dual inverse cone is different. If the single cone uses a conical cross-sectional shape, the dual inverse cone uses a square cross-sectional shape that extends near the dust bin. According to previous research, the best shape of the cone connected to the dust bin is a cone shape because it can reduce the tangential velocity that occurs in the dust bin [17]. On the contrary, the efficiency in the dual inverse cone fluctuates because possibly the tangential velocity is not constant.

### *3.2.3 Contours and vectors*

Figure 7 shows the static pressure contours of the square cyclone separators with three types of cones. Based on Figure 7, the highest pressure distribution on a single cone occurs at the inlet which is 28.80 Pa and on the cyclone wall towards the dust bin is similar at 10.42 Pa. The pressure contour on this single cone is the same as that on a single cone equipped with a dust bin from the research conducted by Venkatesh *et al.,* (2020) with the highest pressure at the inlet of 619 Pa and the distribution on the lower wall pressure of 236 Pa. The pressure difference is possible because the research by Venkatesh *et al.,* (2020) used an inlet velocity of 20.21 m/s and a body diameter of 200 mm while the present study used an inlet velocity of 12 m/s and a body diameter of 150 mm [18].

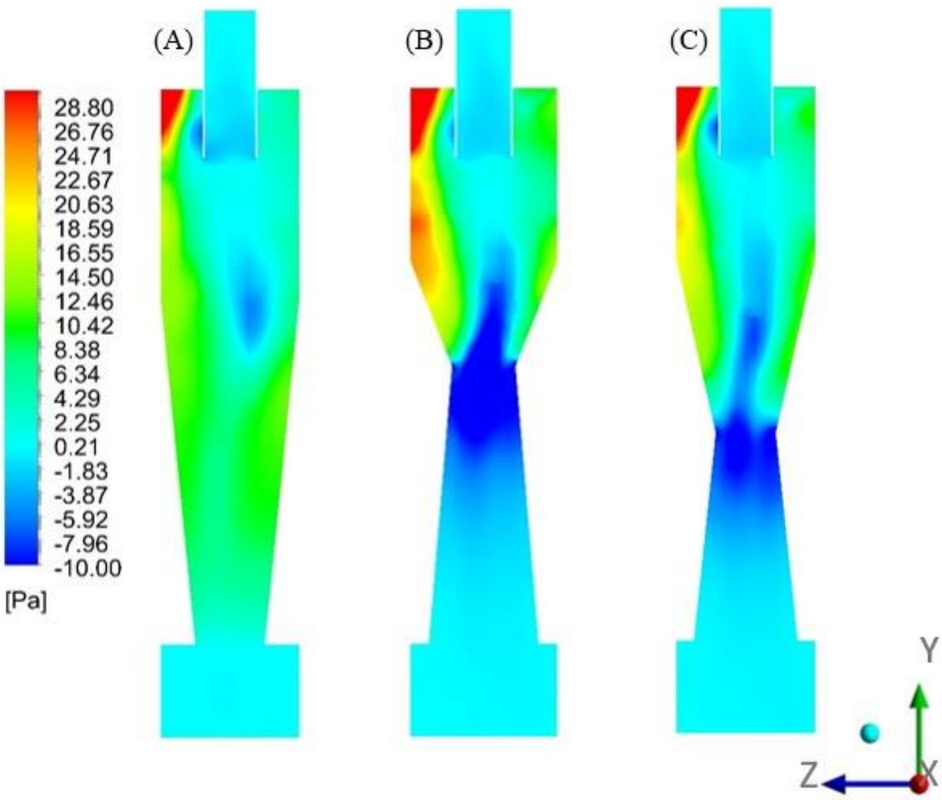


**Fig. 7.** Static pressure contours at 12 m/s inlet velocity and 5 µm particle size of A) Single cone, B) Dual inverse cone 1, C) Dual inverse cone 2

At dual inverse cone 1 the highest pressure also occurs at the inlet which is 28.80 Pa, but at the bottom of the inlet, the pressure that occurs tends to be still high at 24.71 Pa. At dual inverse cone 2, the inlet section experiences a pressure of 28.80 Pa and below the inlet experiences a pressure of 20.63 Pa. Unlike the single cone where the pressure distribution is almost the same, the dual inverse on the upper body wall of the cyclone experience high pressure and at the change of cone shape occur at -10 Pa. This finding is different from the pressure contours on the dual inverse cone conducted by Fatahian *et al.,* (2020) in which the upper body wall of the cyclone experienced the same pressure distribution [9]. It is possible because a dustbin was not used in the study. Moreover, supported by another research which states that a cone or narrow part in the cyclone geometry affects the air residence time, resulting in particles colliding with each other and causing heat transfer on the upper body wall of the cyclone [19]. This is in line with the present study, that the dual inverse cone pressure distribution is higher than the other variation due to a significant narrowing of the cone geometry. High pressure on the cyclone geometry will cause a decrease in collection efficiency [20].

Figure 8 shows the tangential velocity contours of the square cyclone separators with three types of cones. The appearance of the tangential velocity contours in Figure 8 is similar in the upper part of the cyclone. The dual inverse cone experiences a tangential velocity of around 7.66 m/s, while tangential velocity takes place in the single cone in the range of 3.06 m/s. Judging from the tangential velocity distribution, the tangential velocity of the single cone is lower than that of the dual inverse cone, even in the dust bin the tangential velocity is more evenly distributed by 3.83 m/s on the single cone than that of the dual inverse cone. Previous research states that the lower the tangential velocity, the greater the efficiency obtained [17].

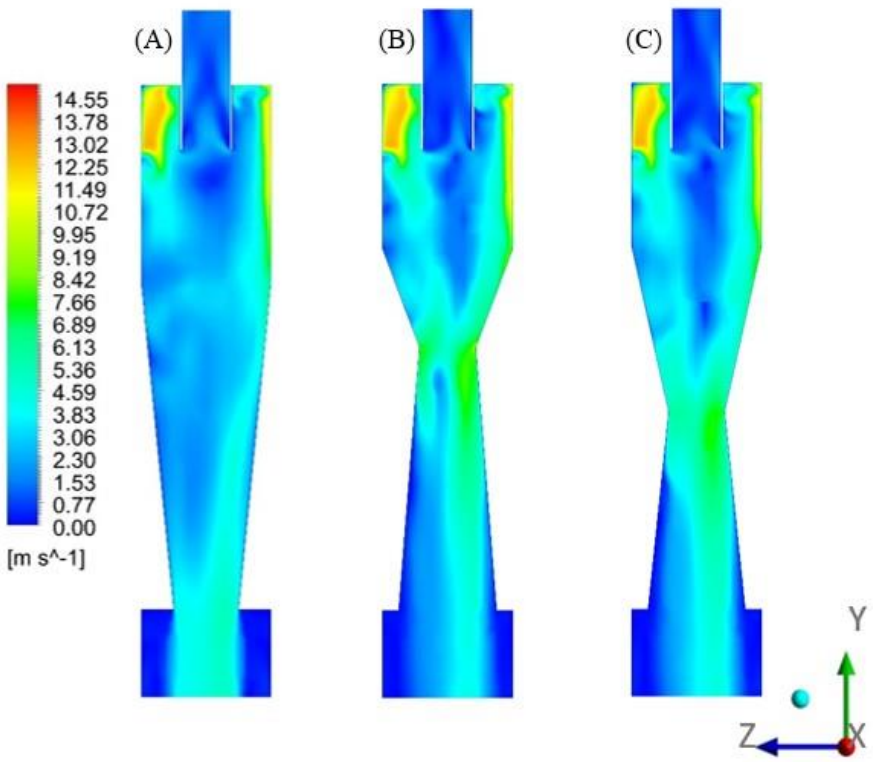


**Fig. 8.** Tangential velocity contours at 12 m/s inlet velocity and 5 µm particle Size of A) Single cone, B) Dual inverse cone 1, C) Dual inverse cone 2

Figure 9 shows the flow vector in cyclone geometry and Figure 10 shows the flow vector of cyclone inlet.

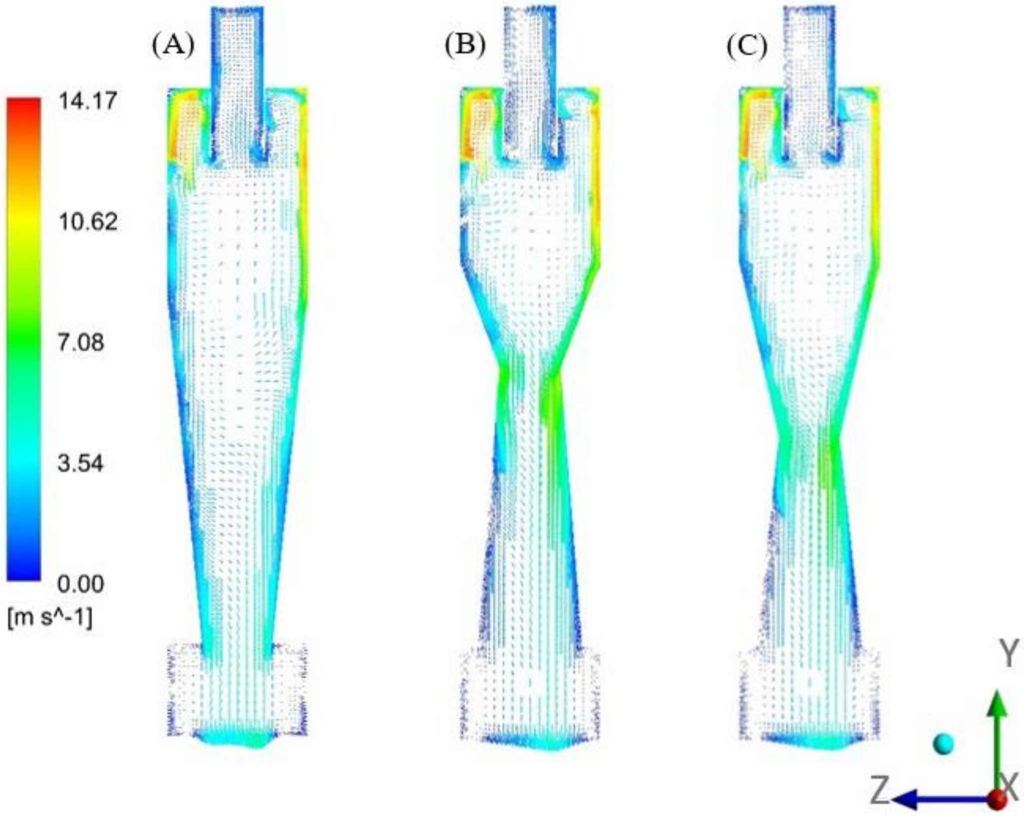


**Fig. 9.** Flow vector in cyclone geometry at 12 m/s inlet velocity and 5 µm particle size A) Single cone, B) Dual inverse cone 1, C) Dual inverse cone 2

In Figure 9, the flow direction of the particle entry vector at the inlet shows the same vector as the findings by Su *et al.,* (2011) that at the inlet without variation there was a parallel direction and turbulence at the edge of the cyclone wall [21]. The direction of flow towards the dust bin of the single cone has a more even flow direction than the dual inverse cone which tends to be in the x+ direction, as shown in Figure 10.

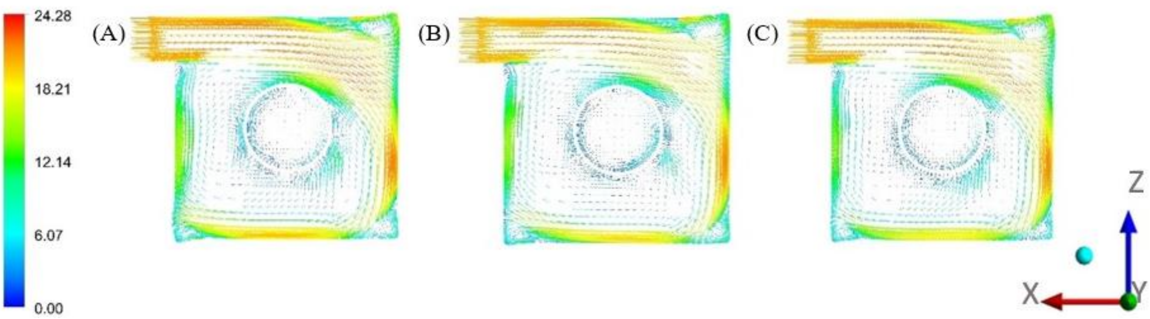


**Fig. 10.** Flow vector of cyclone cross section (y = 1/2h) at 12 m/s inlet velocity and 5 µm particle size A) Single cone, B) Dual inverse cone 1, C) Dual inverse cone 2

### *3.3 Determination of the Best Cone Variation Type*

The determination of the best cone geometry among the three cones: single cone, dual inverse cone 1, and dual inverse cone 2 are based on Table 7:

**Table 7**
Comparison of CFD simulation results for each cone variation

| No. | Aspect | Cone variation | | |
|---|---|---|---|---|
| | | **Single cone** | **Dual inverse cone 1** | **Dual inverse cone 2** |
| 1 | Pressure drop (Pa) (at 28 m/s) | 188.50 | 522.13 | 358.97 |
| 2 | Efficiency (%) (at 28 m/s) | 85.73 | 89.10 | 86.40 |
| | Efficiency in the range of 12 - 28 m/s | More stable | Fluctuating | Fluctuating |
| 3 | Efficiency (%) (50 µm) | 85.51 | 85.68 | 86.27 |
| | Efficiency in the range of 5-50 µm | More stable | Unstable | Fluctuating |
| 4 | Static pressure contour on the cyclone body | Low and uniform (10.42 pa) | Higher at the top of the cone (22.67 pa) | Higher at the top of the cone (18.59 pa) |
| 5 | Tangential velocity contour on the cyclone body | Low and uniform (3.06 m/s) | Higher on the inverse cone (6.13 m/s) | Higher on the inverse cone (6.13 m/s) |
| 6 | Flow vector in cyclone geometry | Centred on the bin | Tends to the right side (x+) | Tends to the right side (X+) |
| 7 | Flow vector of cyclone inlet | Parallel | Parallel | Parallel |

Based on Table 7, it is known that of the seven specified aspects, the single cone fulfils more aspects better than the dual inverse cones with mainly its much lower pressure drop. At an inlet velocity of 28 m/s, the single cone has a much lower value than the other two cone variations, where the double inverse cone 1 and dual inverse cone 2 have a pressure drop value much greater than the single cone value, which is 2.77 and 1.9 times respectively. Meanwhile, the efficiency of the three cone types does not show any significant difference. At an inlet velocity of 28 m/s, the difference in efficiency of single cone 1 compared to double inverse cone 1 and double inverse cone 2 is only 3.96 % and 0.82 %, respectively. Moreover, the efficiency of the single cone in the range of 5-50 µm particle size is the most stable compared to the others. In addition, for a particle size of 50 µm, the efficiencies of the three cone variations are almost equal, with very small differences, from 0.2 % to 0.8 %. Furthermore, static pressure contour and tangential velocity of the cyclone body as well as the flow vector in cyclone geometry as depicted in Figure 7, Figure 8, Figure 9, and Figure 10 further explain that the single cone is considered better than the dual inverse cones.

## 4. Conclusions

Based on the results and discussion, from the seven aspects, a single cone fulfils more aspects better than the dual inverse cones, including the lowest pressure drop of 188.5 Pa, the lowest static pressure contour of 10.42 Pa, the lowest tangential velocity contour of 3.06 m/s, the vector flow direction of the cyclone geometry in the centre of the bin, and the vector flow direction is parallel. Considering its dominantly lowest pressure drop and competitive efficiency compared to those of the dual inverse cone 1 and the dual inverse cone 2, it can be concluded that the single cone is the best among all cone variations.

**Acknowledgement**

The authors are grateful to the Faculty of Engineering, State University of Yogyakarta, Indonesia, for the financial support through the scheme of Research Group Year 2023, Contract Number: T/10.27/UN34.15/PT.01.02/2023.

## References

[1] Jion, Most Mastura Munia Farjana, Jannatun Nahar Jannat, Md Yousuf Mia, Md Arfan Ali, Md Saiful Islam, Sobhy M. Ibrahim, Subodh Chandra Pal *et al.,* "A critical review and prospect of NO2 and SO2 pollution over Asia: Hotspots, trends, and sources." *Science of The Total Environment* 876 (2023): 162851. https://doi.org/10.1016/j.scitotenv.2023.162851

[2] Gao, Yi, Meigen Zhang, Jia Guo, and Liren Xu. "Impact of the oxidation of SO2 by NO2 on regional sulfate concentrations over the North China Plain." *Atmospheric Pollution Research* 13, no. 3 (2022): 101337. https://doi.org/10.1016/j.apr.2022.101337

[3] Wang, Chao, Xiaowei Liu, Dong Li, Junping Si, Bo Zhao, and Minghou Xu. "Measurement of particulate matter and trace elements from a coal-fired power plant with electrostatic precipitators equipped the low temperature economizer." *Proceedings of the Combustion Institute* 35, no. 3 (2015): 2793-2800. https://doi.org/10.1016/j.proci.2014.07.004

[4] Bian, Jiawei, Hai Zhao, Bohan Wang, Bingqiang Han, Hao Ling, and Feng Ju. "Emission characteristics of condensable particulate matter (CPM) from FCC flue gas." *Science of The Total Environment* 882 (2023): 163533. https://doi.org/10.1016/j.scitotenv.2023.163533

[5] Liang, Bin, Haolong Bai, Liangliang Fu, and Dingrong Bai. "Characteristics of the particulate matter and its toxic substances from different stationary coal-fired sources." *Fuel* 334 (2023): 126594. https://doi.org/10.1016/j.fuel.2022.126594

[6] Jaworek, A., A. T. Sobczyk, A. Marchewicz, A. Krupa, and T. Czech. "Particulate matter emission control from small residential boilers after biomass combustion. A review." *Renewable and Sustainable Energy Reviews* 137 (2021): 110446. https://doi.org/10.1016/j.rser.2020.110446

[7] Gao, Xiang, Jinfeng Chen, Jianmei Feng, and Xueyuan Peng. "Numerical investigation of the effects of the central channel on the flow field in an oil–gas cyclone separator." *Computers & Fluids* 92 (2014): 45-55. https://doi.org/10.1016/j.compfluid.2013.11.001

[8] Elsayed, Khairy, and Chris Lacor. "The effect of cyclone vortex finder dimensions on the flow pattern and performance using LES." *Computers & Fluids* 71 (2013): 224-239. https://doi.org/10.1016/j.compfluid.2012.09.027

[9] Fatahian, Hossein, Ebrahim Hosseini, and Esmaeel Fatahian. "CFD simulation of a novel design of square cyclone with dual-inverse cone." *Advanced Powder Technology* 31, no. 4 (2020): 1748-1758. https://doi.org/10.1016/j.apt.2020.02.007

[10] Fatahian, Esmaeel, Hossein Fatahian, Ebrahim Hosseini, and Goodarz Ahmadi. "A low-cost solution for the collection of fine particles in square cyclone: A numerical analysis." *Powder Technology* 387 (2021): 454-465. https://doi.org/10.1016/j.powtec.2021.04.048

[11] Elsayed, Khairy, and Chris Lacor. "The effect of the dust outlet geometry on the performance and hydrodynamics of gas cyclones." *computers & fluids* 68 (2012): 134-147. https://doi.org/10.1016/j.compfluid.2012.07.029

[12] Elsayed, Khairy, and Chris Lacor. "Optimization of the cyclone separator geometry for minimum pressure drop using mathematical models and CFD simulations." *Chemical Engineering Science* 65, no. 22 (2010): 6048-6058 https://doi.org/10.1016/j.ces.2010.08.042.

[13] Mothilal, T., K. Pitchandi, V. Velukumar, and K. Parthiban. "CFD and statistical approach for optimization of operating parameters in a tangential cyclone heat exchanger." *Journal of Applied Fluid Mechanics* 11, no. 2 (2018): 459-466. https://doi.org/10.29252/jafm.11.02.27791

[14] Fatahian, Hossein, Esmaeel Fatahian, and Majid Eshagh Nimvari. "Improving efficiency of conventional and square cyclones using different configurations of the laminarizer." *Powder technology* 339 (2018): 232-243. https://doi.org/10.1016/j.powtec.2018.08.038

[15] Zhang, Zihui, Sijie Dong, Kejun Dong, Li'an Hou, Wenzheng Wang, Yi Wei, and Bo Wang. "Experimental and numerical study of a gas cyclone with a central filter." *Particuology* 63 (2022): 47-59. https://doi.org/10.1016/j.partic.2021.04.014

[16] Sardar, Rajdeep, Jinho Oh, Mirae Kim, Jung-Eon Lee, Seungho Kim, and Kyung Chun Kim. "The Effect of Inlet Velocity, Gas Temperature and Particle Size on the Performance of Double Cyclone Separator." *Chemical Engineering and Processing-Process Intensification* (2023): 109469. https://doi.org/10.1016/j.cep.2023.109469

[17] Obermair, Stefan, Jakob Woisetschläger, and Gernot Staudinger. "Investigation of the flow pattern in different dust outlet geometries of a gas cyclone by laser Doppler anemometry." *Powder Technology* 138, no. 2-3 (2003): 239-251. https://doi.org/10.1016/j.powtec.2003.09.009

[18] Venkatesh, S., M. Sakthivel, H. Saranav, N. Saravanan, M. Rathnakumar, and K. K. Santhosh. "Performance investigation of the combined series and parallel arrangement cyclone separator using experimental and CFD approach." *Powder Technology* 361 (2020): 1070-1080. https://doi.org/10.1016/j.powtec.2019.10.087

[19] Syamsudin, Ferrianto Falikh, Maridjo Maridjo, and Ika Yuliyani. "Pengaruh Penggunaan Rasio Geometri High Efficiency Stairmand terhadap Efisiensi Pengumpulan Top Cyclone Separator." *Jurnal Teknik Energi* 12, no. 1 (2023): 19-23. https://doi.org/10.35313/energi.v12i1.5001

[20] Hoffmann, A. C., and L. E. Stein. "Gas Cyclones and Swirl Tubes.-Berlin Heidelberg New York: Springer." (2008).

[21] Su, Yaxin, Anqiao Zheng, and Bingtao Zhao. "Numerical simulation of effect of inlet configuration on square cyclone separator performance." *Powder technology* 210, no. 3 (2011): 293-303. https://doi.org/10.1016/j.powtec.2011.03.034